

OPEN ACCESS

EDITED BY

Igor Timofeev,
Laval University, Canada

REVIEWED BY

Gert Pfurtscheller,
Graz University of Technology, Austria
Abdulkhaim Al-Ezzi,
Huntington Medical Research Institutes,
United States

*CORRESPONDENCE

MariNieves Pardo-Rodriguez
✉ mnnipi@yahoo.com.mx
Erik Bojorges-Valdez
✉ erik.bojorges@ibero.mx

RECEIVED 19 June 2025

ACCEPTED 10 September 2025

PUBLISHED 29 September 2025

CITATION

Pardo-Rodriguez M, Bojorges-Valdez E,
Arias-Carrion O and Yanez-Suarez O (2025)
Conscious breathing enhances bidirectional
cortical-autonomic modulation: dynamics of
EEG band power and heart rate variability.
Front. Syst. Neurosci. 19:1650475.
doi: 10.3389/fnsys.2025.1650475

COPYRIGHT

© 2025 Pardo-Rodriguez, Bojorges-Valdez,
Arias-Carrion and Yanez-Suarez. This is an
open-access article distributed under the
terms of the [Creative Commons Attribution
License \(CC BY\)](https://creativecommons.org/licenses/by/4.0/). The use, distribution or
reproduction in other forums is permitted,
provided the original author(s) and the
copyright owner(s) are credited and that the
original publication in this journal is cited, in
accordance with accepted academic practice.
No use, distribution or reproduction is
permitted which does not comply with these
terms.

Conscious breathing enhances bidirectional cortical-autonomic modulation: dynamics of EEG band power and heart rate variability

MariNieves Pardo-Rodriguez^{1*}, Erik Bojorges-Valdez^{1*},
Oscar Arias-Carrion² and Oscar Yanez-Suarez³

¹Engineering Studies for Innovation, Universidad Iberoamericana Ciudad de México, Mexico City, Mexico, ²División de Neurociencias Clínica, Instituto Nacional de Rehabilitación Luis Guillermo Ibarra Ibarra, Mexico City, Mexico, ³Neuroimage Research Laboratory, Universidad Autónoma Metropolitana - Iztapalapa, Mexico City, Mexico

Introduction: The mechanisms by which conscious breathing influences brain-body signaling remain largely unexplored. Understanding how controlled breathing modulates neural and autonomic activity can offer insights into self-regulation and adaptive physiological control. This study investigates how conscious breathing affects cortical-autonomic communication by analyzing bidirectional interactions between EEG band power time series (BPTs), heart rate variability (HRV), and breathing signals.

Methods: Data were collected from fifteen healthy subjects during three experimental conditions: a spontaneous breathing state (Rest) and two controlled breathing tasks (CBT 1 and CBT 2). EEG recordings were analyzed to compute BPTs across the δ , θ , α , β , and γ frequency bands, while HRV and breathing signals were derived from ECG data. Cross-spectrum analysis and Granger causality tests were performed between HRV and BPTs. To further investigate directional interactions, Granger-causal relationships were explored between components of the BPTs extracted using empirical mode decomposition and the HRV and breathing signals.

Results: Bidirectional Granger-causal relationships were found between neural and autonomic systems, emphasizing the dynamic interaction between the brain and body. Specific BPTs components mediated neural-autonomic communication, with one component consistently aligning with the frequency of conscious breathing (~ 0.05 Hz) during the CBTs. Cross-spectral peaks at this frequency and its harmonics highlight the role of respiratory entrainment in optimizing neuro-autonomic synchronization. Frequency-specific mechanisms observed in both fast and slow components reflect the complex regulation of autonomic functions through cortical modulation. The most prominent causal effects were observed in the γ band, suggesting its pivotal role in dynamic autonomic regulation, potentially acting as a communication pathway between the brain and body.

Discussion: Our results demonstrate that conscious breathing enhances bidirectional cortical-autonomic modulation through frequency-specific dynamic neural mechanisms. These findings support a closed-loop model of physiological regulation driven by neural-respiratory entrainment and suggest that respiration can serve as a top-down mechanism for autonomic control. By clarifying how conscious breathing shapes brain-body dynamics, this work lays the foundation for research on neural self-regulation and supports the

development of non-pharmacological interventions for improving mental and physiological health.

KEYWORDS

neuromodulation, autonomic regulation, entrainment, heart rate variability (HRV), EEG-band power time series, breathing, Granger-causal relationship

1 Introduction

Extensive electroencephalography (EEG) research has highlighted that the brain operates with a hierarchical organization, where slower oscillations modulate the amplitude of faster ones, thereby facilitating communication between distant brain areas and enhancing cognitive flexibility in response to internal or external demands (Klimesch, 2013, 2018; Lakatos et al., 2005; Siegel et al., 2012). This modulation supports the redistribution of oscillatory activity across frequency bands, maintaining functional equilibrium and optimizing information processing.

More recently, the concept of neuronal entrainment *i.e.*, the synchronization of brain oscillations with rhythmic inputs has emerged as a key factor in influencing the temporal dynamics of cortical activity. Entrainment enhances interregional communication, optimizes information flow, and supports adaptive responses to environmental changes (Lakatos et al., 2019). Studies in animal models (Tort et al., 2018; Zhong et al., 2017) and humans with epilepsy (Herrero et al., 2018; Zelano et al., 2016) using intracranial recordings have shown that respiratory activity can phase-lock with neural oscillations and modulate the amplitude of higher-frequency rhythms. Furthermore, coupling between breathing and neural rhythms has been shown to promote parasympathetic dominance, improving information processing while reducing stress (Benson et al., 1974; Noble and Hochman, 2019). This dynamic interplay between neural activity and the autonomic system suggests that consciously modulating breathing could enhance both neural communication and autonomic regulation.

The autonomic nervous system (ANS) plays a crucial role in maintaining bodily regulation, balancing excitation and inhibition of involuntary signals throughout the body and brain (Saper, 2002). A key measure of ANS activity, heart rate variability (HRV), reflects its capacity to adapt to changing internal and external conditions, with increased variability indicating more robust autonomic control. HRV has been linked to cognitive and emotional performance, and has proven valuable in exploring the dynamics of autonomic regulation (Faes et al., 2017; Klimesch, 2018; Noble and Hochman, 2019; Pardo-Rodriguez et al., 2021a; Zaccaro et al., 2018).

Breathing directly influences HRV, with specific respiratory patterns shaping autonomic responses and overall physiological balance (Critchley et al., 2015). HRV is associated with respiratory sinus arrhythmia (RSA), a phenomenon where heart rate reflects the phases of breathing, further demonstrating the interconnectedness of autonomic processes (Klimesch, 2018; Porges, 2007). Conscious control of breathing such as slow, deep, or rhythmic patterns can enhance parasympathetic activation, reduce stress, and increase HRV, promoting relaxation and improving psychophysiological states (Ashhad et al., 2022;

Benson et al., 1974; Noble and Hochman, 2019; Weng et al., 2021). Notably, breathing at 0.1 Hz (six breaths per minute) induces resonance between respiratory and cardiovascular rhythms, optimizing autonomic function by reinforcing these physiological signals (Ashhad et al., 2022; Mather and Thayer, 2018; Noble and Hochman, 2019; Zaccaro et al., 2018). This process is increasingly understood to involve the brain-heart axis, a complex network of neural, mechanical, and biochemical pathways linking central and autonomic functions (Valenza et al., 2025). This resonance enhances synchronization between the cardiovascular and respiratory systems, promoting autonomic control (Ashhad et al., 2022; Carnevali et al., 2013; Noble and Hochman, 2019).

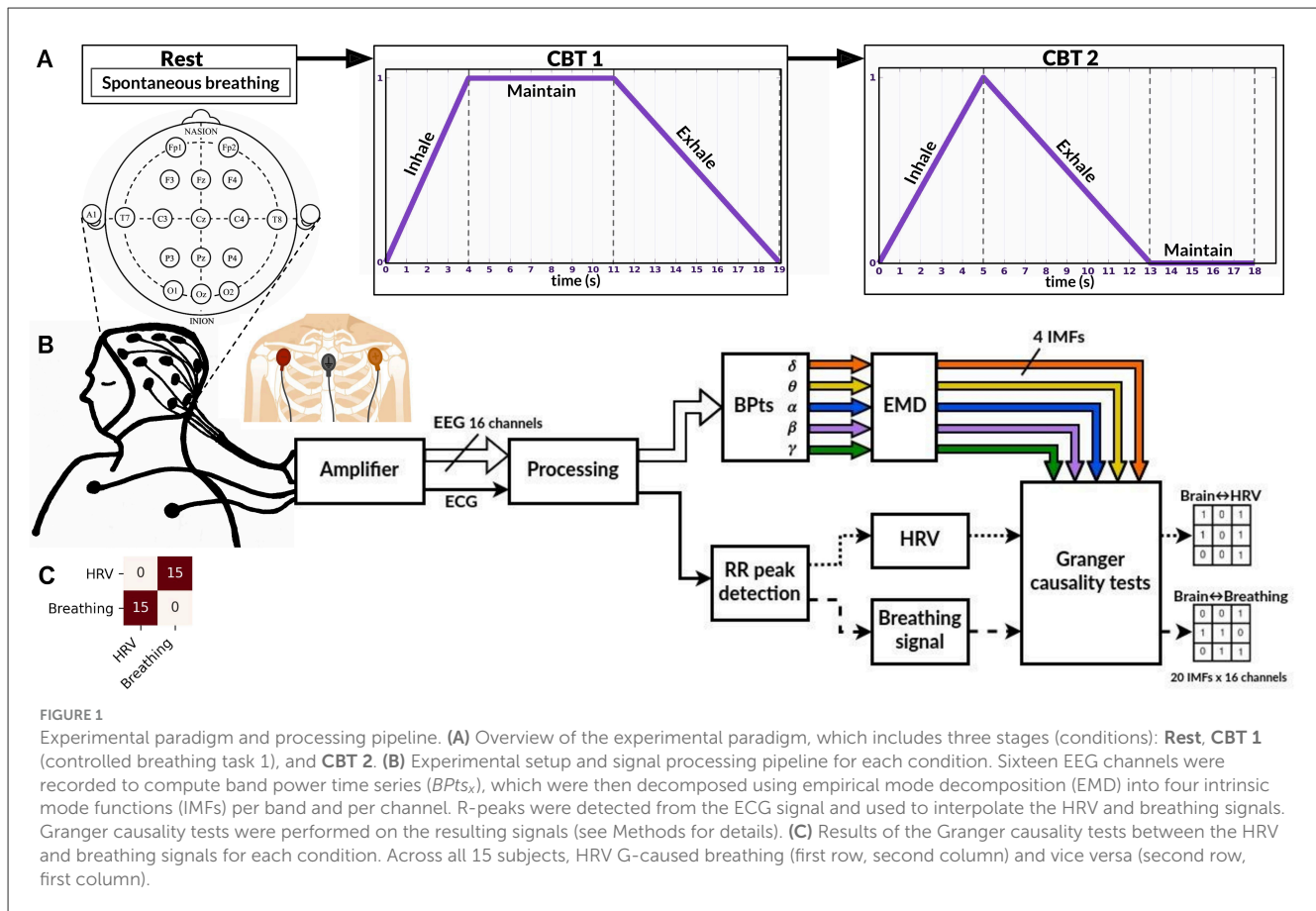
Despite the growing popularity of breath-focused interventions in clinical and wellness contexts, the mechanisms by which specific breathing patterns could influence both neural and autonomic systems remain poorly understood. Recent studies have begun exploring how conscious breathing, combined with interoceptive attention, may influence brain oscillations and support autonomic regulation (Critchley and Garfinkel, 2015; Herrero et al., 2018; Pardo-Rodriguez et al., 2021a; Porges, 2007). The present study seeks to address this gap by examining how conscious modulation of breathing influences EEG oscillations and autonomic regulation.

Building on the concept of neuronal entrainment proposed by Lakatos et al. (2019), we suggest the brain uses breathing rhythms as pacing signals to modulate its oscillatory activity. Voluntary changes in breathing may influence vagal afferents by coupling respiration, baroreceptor inputs and O₂ and CO₂ exchange, inducing phase shifts that align both EEG activity and HRV with the breathing cycle. This modulation could recruit cortical rhythms at multiple frequencies, harmonically aligned with breathing, thereby influencing cortical temporal dynamics. In line with Lakatos et al. (2005) hierarchical oscillation theory, we propose that low-frequency respiratory rhythms modulate the amplitude of higher-frequency neural oscillations, enhancing interregional cortical communication and supporting cognitive flexibility. We thus hypothesize that conscious modulation of breathing enhances brain-body communication, improving neural synchronization and autonomic regulation compared to spontaneous breathing.

2 Materials and methods

2.1 Data

Data were collected from fifteen healthy subjects (seven female), aged 24 ± 3 years. Inclusion criteria were: normal body-mass index, no regular practice of an aerobic exercise, non-smoker, non-medicated, no known neuropathies or cardiovascular conditions, and no consumption of coffee or stimulating beverages two hours before the recordings. Subjects participated voluntarily



after providing informed consent and received no monetary compensation. The experimental protocol followed the Declaration of Helsinki and had the approval of the University’s Ethics Committee under record number 221. Recordings were scheduled between 10h 00 to 12h 00 to minimize any circadian influences on autonomic functions, as HRV can fluctuate throughout the day. Stimulus presentation and recording synchronization were done using BCI2000 software (Schalk et al., 2004). Signals were recorded using a g.USBamp (g.tec, Austria) amplifier at 1,200 samples per second, with a 60 Hz notch filter activated and the g.SCARABEO (g.tec, Austria) active electrode system. EEG signals were recorded from 16 channels placed according to the standard 10-20 system: $Fp1$, $Fp2$, $F3$, Fz , $F4$, $C3$, Cz , $C4$, $T7$, $T8$, $P3$, Pz , $P4$, $O1$, $O2$, and Oz . The reference used was $A1$ and ground at Fpz . ECG signals were recorded by placing a pair of electrodes on the chest just below the left and right clavicles, and ground over the manubrium of the sternum (Figure 1B). Although this setup is not a clinical standard for ECG recordings, it was sufficient for detecting R-peaks, which are necessary for HRV estimation. Subjects were comfortably seated in a recliner armchair with head support from the moment they entered the recording area. Electrode setup took approximately 20 min, allowing for the transient phase of adaptation to pass and ensuring that participants’ autonomic tone was at a relatively stable baseline before recordings began. These experiments were conducted at the Center for Well-Being (CBU, Centro del Bienestar Universitario) of Universidad Iberoamericana Ciudad de Mexico.

Although our sample size ($n = 15$) is relatively small, the consistency of directional interactions across nearly all

participants suggests robust effects. Comparable studies in brain-heart dynamics have reported similar results with similar sample sizes (De la Cruz-Armenta et al., 2017; Faes et al., 2017; Pardo-Rodriguez et al., 2019; Umeno et al., 2002; Valenza et al., 2016). Nonetheless, expanding the participant pool in future research is essential to capture a broader variability in physiological responses and to better identify potential outliers. This would strengthen the generalizability of the observed effects and support more robust statistical inference.

2.2 Experimental design

The experimental protocol consisted of three conditions, depicted on Figure 1A, which were applied uniformly across all subjects. This design allowed us to compare spontaneous and consciously regulated breathing states to investigate whether specific breathing patterns enhance neuralautonomic coupling, as hypothesized. During all conditions, subjects remained in the same seated position with their eyes closed.

- **Resting condition (Rest):** Subjects were instructed to listen to an audio recording of “The Origin of Evil” by Leon Tolstoi, which lasted 6 min and 53 s (audio available at: [The Origin of Evil](#)). No instructions regarding breath control were given, therefore subjects engaged in spontaneous breathing during this phase.

- **CBT training 1:** Subjects were instructed and demonstrated how to perform a controlled breathing task (CBT), guided by an auditory cue (audios available at: [CBTs training](#)). The task was performed exclusively using nasal breathing. The cue indicated inhalation with an increasing frequency tone, maintenance by keeping a constant tone, and exhalation with a decreasing frequency tone. Data was recorded during this phase, but was not included in the analysis. For this training, subjects practiced a short, two-minute version of the CBT described below.
- **Controlled breathing task 1 (CBT 1):** Once subjects were able to synchronize their breathing with the auditory cue, they were instructed to perform **CBT 1**. This task consisted of breathing cycles with 4 seconds of inhalation, 7 s of breath-holding, and 8 s of exhalation. The task lasted 10 min, during which 32 cycles were performed.
- **CBT training 2:** The second controlled breathing training session was conducted in the same manner as described above for the subsequent and final condition. The task was performed exclusively using nasal breathing. Data was recorded during this phase, but was not included in the analysis. Once again, subjects practiced a short, two-minute version of the new CBT described below.
- **Controlled breathing task 2 (CBT 2):** CBT 2 consisted of breathing cycles with 5 s of inhalation, 8 s of exhalation, and 5 s of breath-holding. This task also lasted 10 min, with 34 cycles performed.

These breathing protocols were selected to approximate a lower harmonic of the well-studied 0.1 Hz resonance frequency (i.e., ~ 0.05 Hz), which has been associated with enhanced parasympathetic activation and autonomic regulation (Russo et al., 2017; Zaccaro et al., 2018). The 4-7-8 pattern is a well-established pranayama-based technique with documented effects on HRV, blood pressure, and stress reduction (Vierra et al., 2022). The 5-8-5 pattern, while less common in clinical studies, was designed to maintain a comparable cycle duration while modifying the phase distribution, consistent with slow-breathing principles used in respiratory training (Bhargava et al., 1988).

Although no direct respiratory signal (e.g., nasal thermistor) was recorded, participants were instructed to breathe exclusively through the nose. This was continuously monitored by the experimenter throughout the sessions. While slow, rhythmic breathing can be achieved via either the mouth or nose, nasal airflow has distinct neural effects that oral breathing lacks. Specifically, it has been shown to entrain cortical and limbic oscillations, via olfactory pathways, linked to the modulation of emotional states (Herrero et al., 2018; Pfurtscheller et al., 2025; Tort et al., 2025; Zelano et al., 2016).

2.3 Signal processing

Figure 1B shows the experimental setup and the processing pipeline applied to each condition. Figure 2 provides an example of the signals recorded from one trial. All signals were filtered using a digital band-pass filter with cutoffs at 0.01 Hz and 100 Hz, consisting of a fourth-order

Butterworth high-pass filter and an eighth-order Chebyshev II low-pass filter.

ECG signals were differentially obtained from the chest electrodes, and R-peaks of the QRS complex were identified using Hamilton's algorithm (Hamilton, 2002). HRV was determined from the time differences between these peaks and interpolated to a standard sampling rate of 10 samples per second using cubic interpolation. The breathing signal, derived from the amplitude of the R-peaks, was also interpolated to the same sampling rate using cubic interpolation.

Relative band power time series (BPTs) for the five classical frequency bands (δ (1-4 Hz), θ (4-8 Hz), α (8-12 Hz), β (12-30 Hz), and γ (30-100 Hz)) were estimated for all EEG channels using a sliding window of two seconds with 95% overlap, resulting in a sampling rate of 10 samples per second. The Welch periodogram method was applied to each window, with internal parameters configured to assess a resolution of 0.5 Hz using a half-size window and 95% overlap. Relative power estimates were calculated by integrating the power spectral density (PSD) within each frequency band and normalizing by the total power (Figure 2C). This methodology has been previously described in the work of Pardo-Rodriguez et al. (2021a,b,c). All signals (BPTs, HRV and breathing) were resampled for synchronization over the same temporal axis.

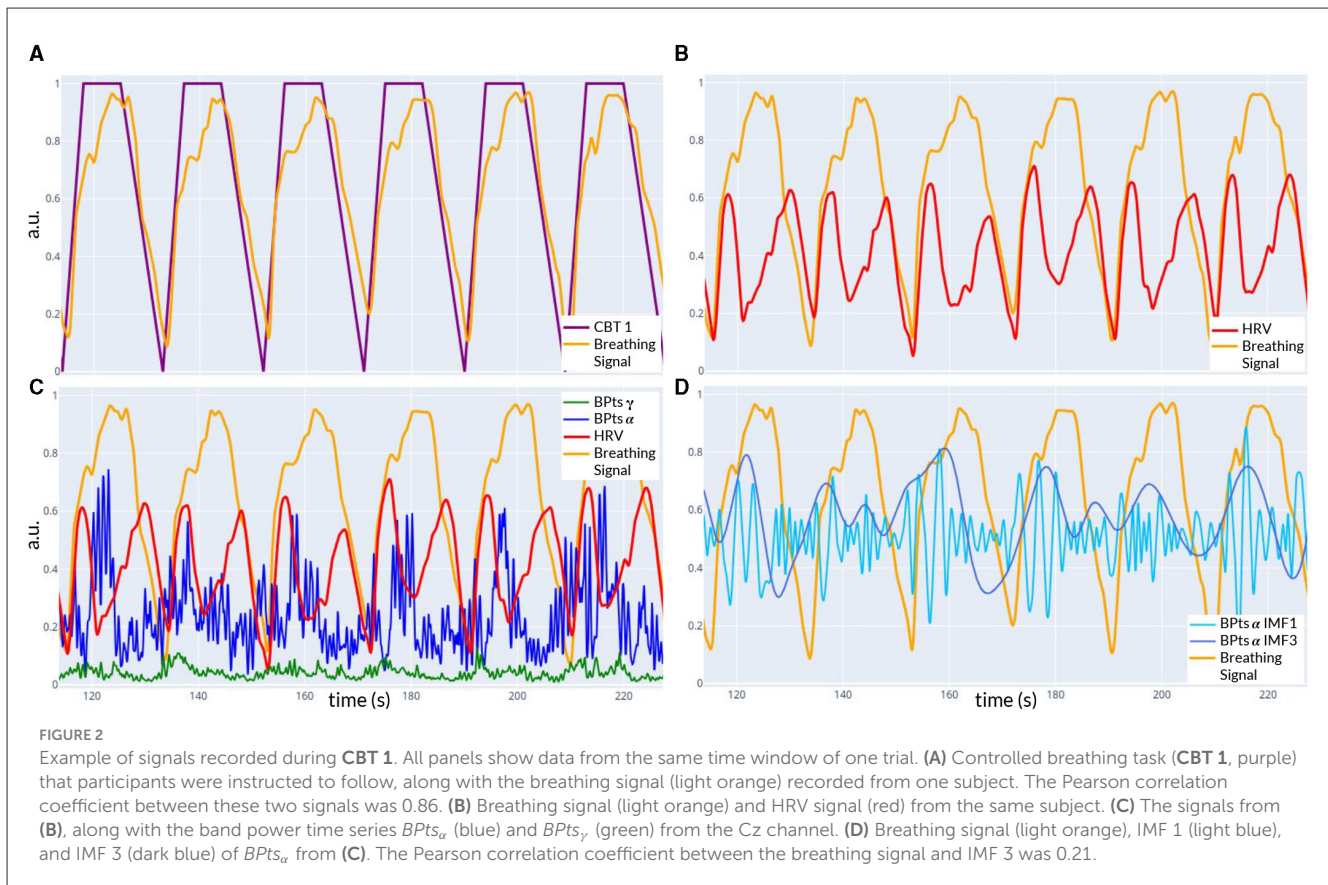
2.4 Analyses

2.4.1 Band power analysis

To assess whether significant changes in band power occurred during the CBTs, between **Rest** vs **CBT1** and **Rest** vs **CBT2**, Shapiro-Walk normality tests were conducted on the data from all subjects, for each band and channel. For each pair of groups (different condition, same band and channel) with normal distributions, a parametric two-tailed t-test was performed. If normality was rejected for one of the groups, a Wilcoxon signed-rank test was used instead. The significance level for all statistical tests was set at 0.025, following a Bonferroni correction to account for multiple comparisons across the different conditions.

2.4.2 Cross-spectrum analysis

Subsequently, the cross-spectrum between the normalized BPTs and HRV signals was computed, yielding a spectral resolution of 0.01 Hz. For each frequency band and EEG channel, the amplitude at 0.05 Hz was compared between **CBT 1** and **Rest**, and the amplitude at 0.06 Hz was compared between **CBT 2** and **Rest**. These frequencies were chosen as they were the closest estimated frequencies to the breathing rate of each CBT. For each condition, band, and channel, normality was assessed using the Shapiro-Walk test. Depending on the outcome, either a paired t-test or a Wilcoxon signed-rank test was applied. Effect sizes were then calculated using Cohens d, based on all data from each CBT compared to **Rest**, along with the corresponding confidence intervals (CIs) and p-values. Values of Cohens d around 0.2 are generally considered small, around 0.5 medium, and 0.8 or higher large, indicating the strength of observed differences between mean cross-spectrum values across conditions.



2.4.3 Empirical mode decomposition (EMD)

Following this, to analyze changes in terms of specific spectral components, four intrinsic mode functions (IMFs) were extracted from the BPTs for each channel and frequency band using empirical mode decomposition (EMD) (Figure 2D). The EMD method (Huang Norden et al., 1998) was chosen for analyzing the BPTs because it is particularly suited for non-stationary and non-linear processes, like BPTs. The Python EMD package was used to compute the decomposition, specifically employing the *emd.sift.sift* function with default parameters (Quinn et al., 2021). Unlike traditional methods such as the STFT (short-time Fourier transform) or filter banks, which assume stationarity, EMD adapts to the data, extracting IMFs that reflect dynamic, time-varying oscillations without predefined frequency limits. This makes EMD ideal for capturing the complex temporal characteristics of the BPTs.

Although EMD can introduce artifacts such as mode mixing, we ensured the reliability of the IMFs chosen by assessing the power spectral density (PSD) of each IMF and verifying the consistency of their bandwidths across subjects. The dominant frequency content of each IMF, identified as the peak frequency and the range exceeding 90% of peak power was calculated across all subjects, channels and bands, separately for each condition. The resulting frequencies were highly stable across tasks, with averaged values as follows: IMF 1 peaked at 0.262 Hz (range: 0.246–0.277 Hz), IMF 2 at 0.136 Hz (0.130–0.142 Hz), IMF 3 at 0.059 Hz (0.057–0.062 Hz), and IMF 4 at 0.026 Hz (0.025–0.027 Hz). Notably, the dominant frequency peaks for each IMF were distinct and showed no overlap.

2.4.4 Causal analysis

Granger causality tests were first performed between each BPTs (per channel) and the HRV signal to capture directional dependencies that may reflect neural-autonomic coupling. Granger causality is a statistical method used to determine whether past values of one time series can help predict future values of another time series (Granger, 1969). The test compares models that predict a signal using its own past values against models that include past values of another signal. If incorporating the second signal improves prediction accuracy significantly ($p < 0.01$), the first signal is said to G-cause the second. However, this causal relationship does not imply a direct physical connection between the signals, just a predictive dependency that underscores some form of functional connectivity. Effect sizes were then calculated using the Odds Ratio (OR), based on all data from each CBT compared to **Rest**, along with the corresponding CIs and p -values. OR values above 1 indicate increased likelihood of positive G-causal relationships during the CBTs compared to **Rest**, whereas values below 1 suggest a decreased likelihood.

Finally, Granger causality tests were also performed between each IMF (by band and channel) and the HRV and breathing signals.

Recent studies have highlighted Partial Directed Coherence (PDC) as a frequency-domain alternative for assessing directional connectivity in EEG, particularly in relation to HRV and event-related desynchronization (Al-Ezzi et al., 2024; Molloy et al., 2023). While Granger causality operates in the time domain and is well-suited for examining short, transient neural-autonomic dynamics,

TABLE 1 Mean relative BPTs differences between Rest and CBT 1 in arbitrary units.

Channel	δ	θ	α	β	γ	Channel	δ	θ	α	β	γ
Fp1	0.026	-0.005	-0.021	-0.000	0.004	Fp2	0.015	-0.009	-0.026	-0.002	0.028
F3	0.026	-0.013	-0.019	-0.000	0.012	F4	0.028	-0.012	-0.025	0.000	0.013
Fz	0.018	-0.010	-0.018	0.001	0.014	Cz	0.010	-0.017**	-0.013	0.007	0.017*
C3	0.022	-0.016**	-0.019*	0.005	0.014	C4	0.028	-0.020**	-0.019**	0.001	0.015
T7	0.000	-0.014**	-0.019*	0.008	0.029**	T8	0.026	-0.021**	-0.031**	0.004	0.029
P3	0.016	-0.012**	-0.030**	0.011*	0.018**	P4	0.019	-0.015**	-0.030**	0.009	0.020**
Pz	-0.003	-0.010	-0.020	0.015**	0.019**	Oz	0.016	-0.014*	-0.051**	0.004	0.051
O1	0.024	-0.017**	-0.053**	0.004	0.048**	O2	0.033	-0.017**	-0.064**	0.004	0.050**

Comparisons were made across the respective frequency band and channel for all subjects, between the two conditions (**Rest** and **CBT 1**) using either a two-tailed t-test or a Wilcoxon signed-rank test, depending on the normality of the data. Significant differences are indicated by * and ** next to each difference, where $p < 0.025$ and $p < 0.01$, respectively. Positive values indicate an increase during **CBT 1**.

TABLE 2 Mean relative BPTs differences between Rest and CBT 2 in arbitrary units.

Channel	δ	θ	α	β	γ	Channel	δ	θ	α	β	γ
Fp1	0.022	0.001	-0.022	-0.002	0.004	Fp2	0.006	0.006	-0.011	0.015	-0.016
F3	0.032	-0.005	-0.024	-0.002	0.003	F4	0.026	-0.002	-0.026	0.000	0.004
Fz	0.011	-0.000	-0.013	0.001	0.004	Cz	0.004	-0.008	-0.008	0.005	0.009
C3	0.019	-0.007	-0.018	0.003	0.004	C4	0.004	-0.006	-0.009	0.005	0.007
T7	0.020	-0.009**	-0.019	-0.001	0.011	T8	0.008	-0.009	-0.030	0.007	0.029
P3	0.027	-0.004	-0.038*	0.005*	0.009	P4	0.015	-0.003	-0.030*	0.007	0.012
Pz	-0.005	-0.001	-0.026	0.010*	0.012*	Oz	0.032	-0.002	-0.051*	0.001	0.034
O1	0.036	-0.005	-0.060*	0.001	0.032	O2	0.039	-0.004	-0.068**	0.002	0.034

Comparisons were made across the respective frequency band and channel for all subjects, between the two conditions (**Rest** and **CBT 2**) using either a two-tailed t-test or a Wilcoxon signed-rank test, depending on the normality of the data. Significant differences are indicated by * and ** next to each difference, where $p < 0.025$ and $p < 0.01$, respectively. Positive values indicate an increase during **CBT 2**.

future work could integrate PDC to explore band-specific or long-range neural-autonomic interactions more precisely.

3 Results

3.1 Band power analysis

Mean BPTs increased in the δ , β , and γ bands during both **CBTs** across nearly all channels when compared to **Rest**, as shown in **Tables 1, 2**. However, these differences were only significant for $BPTs_{\beta}$ at P3 and Pz for both **CBTs**; and for $BPTs_{\gamma}$ at Pz for both **CBTs**, and at Cz, T7, P3, P4, O1 and O2, for **CBT 1**. In contrast, for **CBT 1**, significant decreases in mean BPTs were observed in the θ and α bands from central through occipital channels, excluding Pz. For **CBT 2**, significant decreases were found in $BPTs_{\theta}$ at T7 and in $BPTs_{\alpha}$ at P3, P4, Oz, O1 and O2.

3.2 Cross-spectrum analysis

Figure 3 provides initial evidence of neural and autonomic coupling driven by controlled breathing. The cross-spectrum quantifies the degree to which two signals share spectral power at specific frequencies, reflecting their frequency-domain coherence. In **Figures 3B, C**, the dominant spectral peak is centered at the respective **CBT** frequency, followed by progressively smaller peaks at its harmonics indicating a cyclical interaction likely

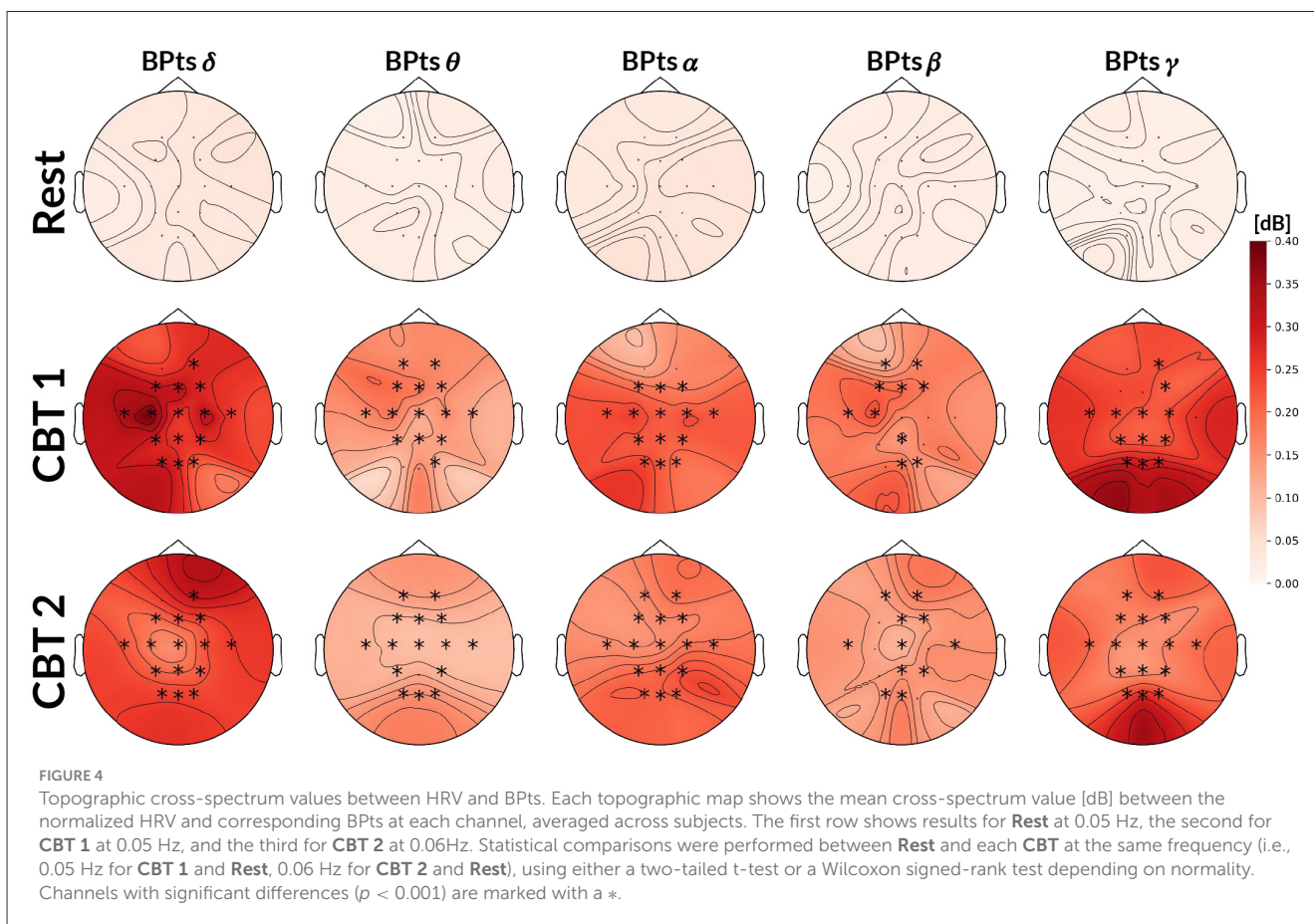
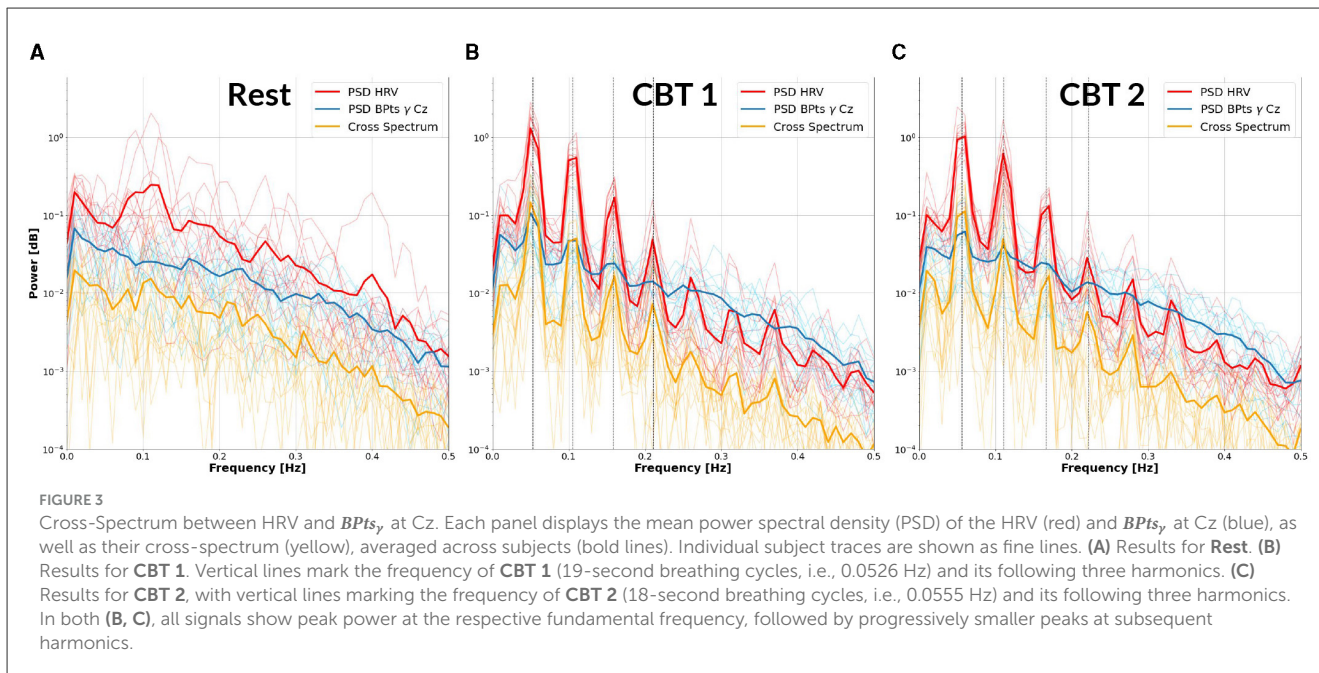
entrained by the breathing pattern. These harmonics are consistent with the periodic structure of the controlled breathing tasks and suggest coherent phase-locking between neural activity and cardiorespiratory rhythms. In contrast, **Figure 3A** shows that during **Rest**, the cross-spectrum is more broadly distributed across frequencies, with no prominent peaks, suggesting the absence of such coupling.

Figure 4 shows that cross-spectrum values between HRV and BPTs during the **CBTs**, at the frequencies closest to the respective breathing rates (*i.e.*, 0.05 Hz for **CBT 1** and 0.06 Hz for **CBT 2**), increased significantly across subjects compared to **Rest**. Effect sizes measured through Cohen’s *d* were 1.37 (95% CI: [1.27, 1.47]; $p < 0.001$) for **CBT 1** vs. **Rest**, and 1.45 (95% CI: [1.34, 1.55]; $p < 0.001$) for **CBT 2** vs **Rest**. This means that controlled breathing was strongly associated with enhanced frequency-specific coupling between neural and autonomic signals.

3.3 Granger causality

3.3.1 BPTs→HRV

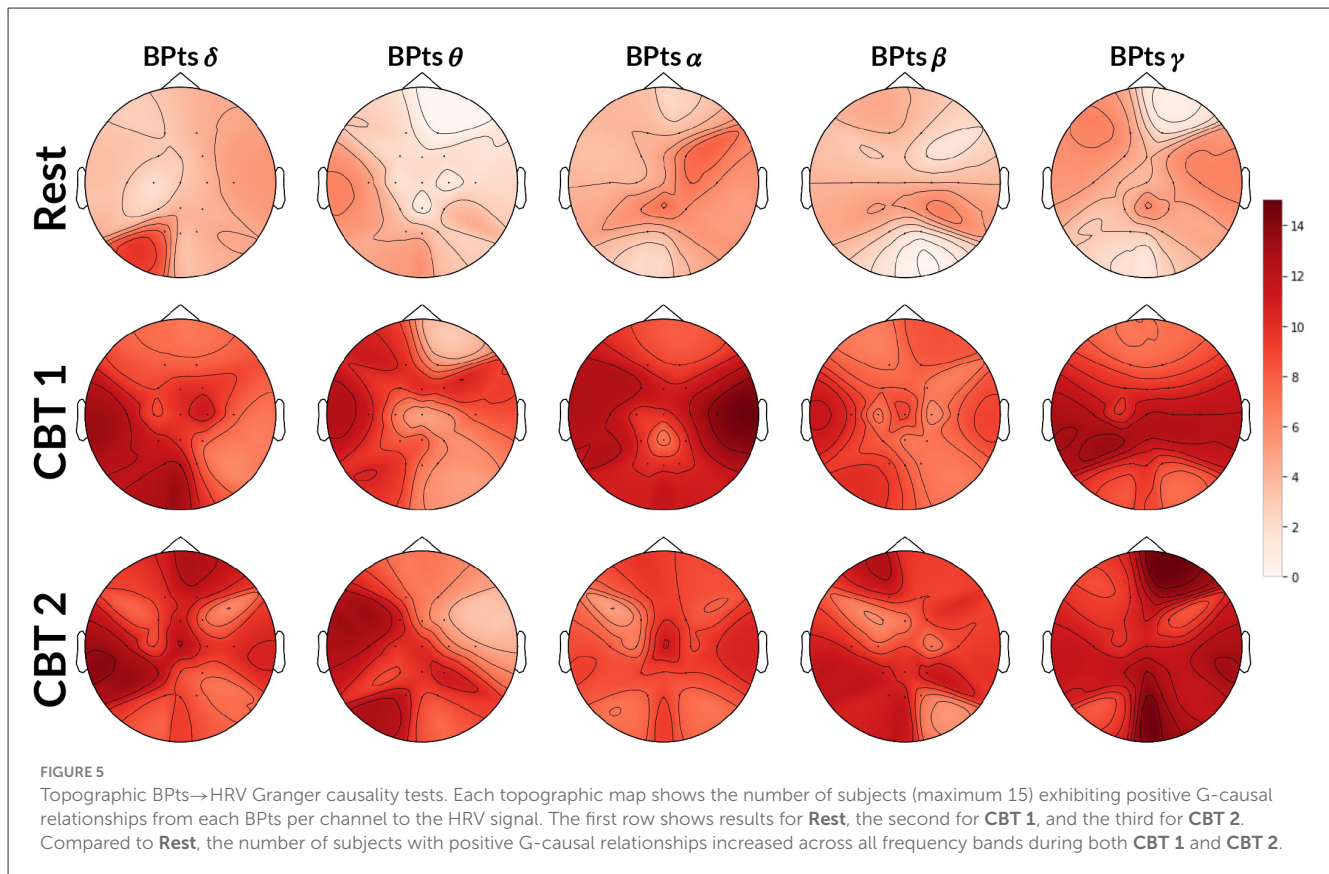
Topographic maps in **Figure 5** show an increase in G-causal relationships from BPTs→HRV across all frequency bands during both **CBTs** compared to **Rest**. The γ band exhibited the highest number of subjects with positive G-causality overall, while the θ band showed the greatest increase relative to **Rest**. Effect size analysis indicated that subjects were 4.74 times more likely



to show positive G-causality during **CBT 1** compared to **Rest** ($OR = 4.74$; 95% CI: [3.89, 5.79]; $p < 0.001$), and 5.13 times more likely during **CBT 2** ($OR = 5.13$; 95% CI: [4.20, 6.27]; $p < 0.001$).

3.3.2 HRV→BPts

Topographic maps in **Figure 6** show a higher total number of G-causal relationships from HRV→BPts during both **CBTs**, with increases observed across all frequency bands compared



to **Rest**. Again, the γ band showed the highest number of subjects with positive G-causality overall, while the θ band showed the greatest relative increase. However, unlike the BPTs→HRV direction, HRV→BPTs already exhibited a higher baseline level of G-causality during **Rest**. As a result, the observed increases during the CBTs, though more numerous in absolute terms, were smaller in relative magnitude. Effect size analysis showed that subjects were 1.93 times more likely to exhibit positive G-causality during **CBT 1** compared to **Rest** ($OR = 1.93$; 95% CI: [1.58, 2.36]; $p < 0.001$), and 2.10 times more likely during **CBT 2** ($OR = 2.10$; 95% CI: [1.71, 2.58]; $p < 0.001$).

To gain finer insight into the spectral components of the BPTs and their relationship with HRV and respiration, we next applied Granger causality analyses to the BPTs decomposed via EMD. For this decomposition analysis, we adopt the terms **brain→body** and **body→brain** to reflect the broader conceptual framing, where “brain” refers to the IMFs of BPTs, and “body” encompasses both HRV and breathing signals. Figure 7 shows results for the **brain→body** direction, while Figure 8 shows the results for the **body→brain** direction.

3.3.3 Brain→body

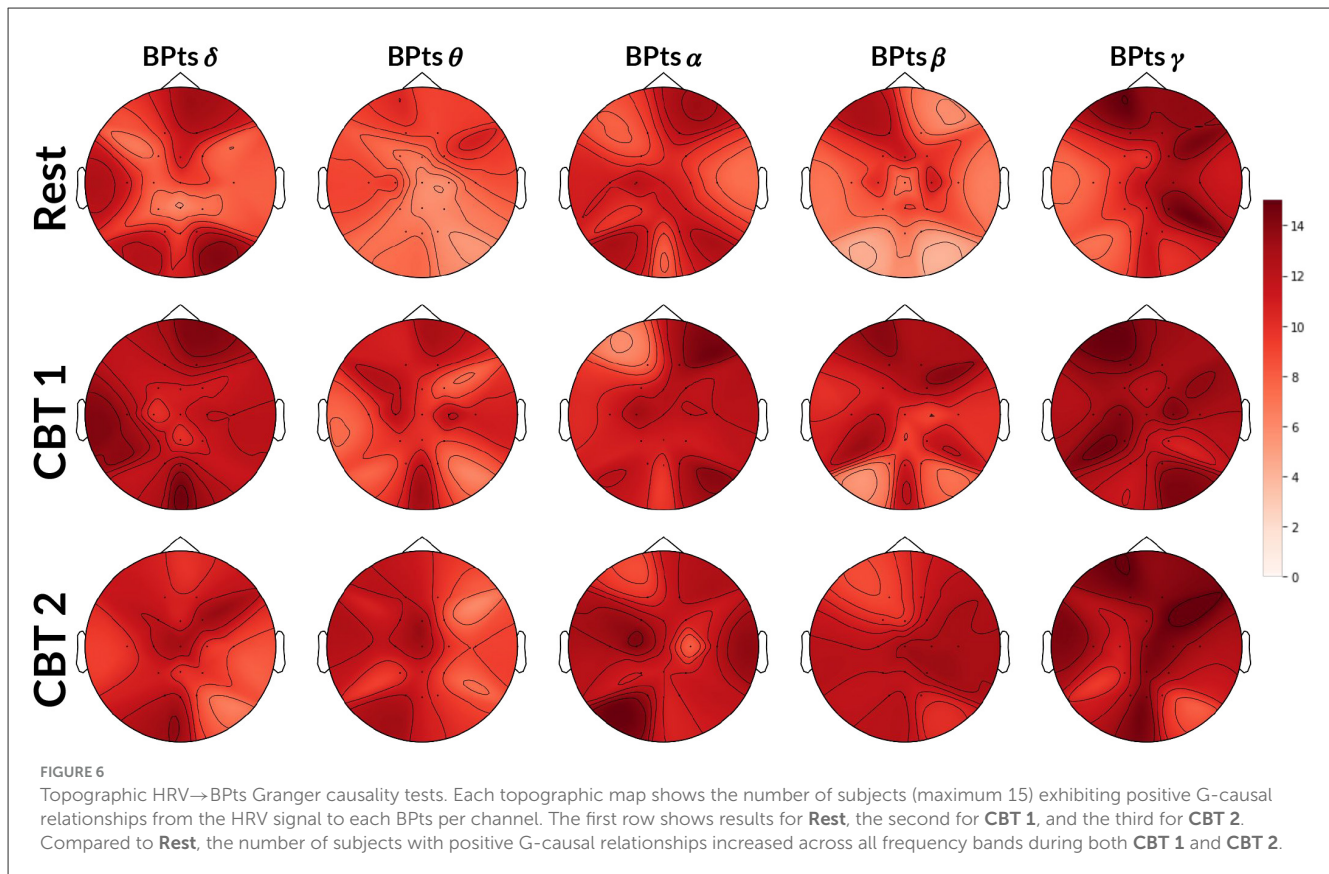
Figure 7 shows that, for both CBTs, G-causal relationships increased for IMF 3 and IMF 4 across all frequency bands compared to **Rest**. The greatest increase was observed for **brain→breathing** relationships on IMF 3, particularly in the δ , α and γ bands, and on IMF 4 in the γ band. Additionally, **brain→HRV** relationships increased for IMF 2 in δ , α and γ bands. In contrast,

G-causal relationships for IMF 1 decreased across most frequency bands, except for γ during **CBT 1**, in the majority of channels. Channel distribution shows that G-causal relationships increased predominantly over central and frontal channels for **brain→HRV** in the β and γ bands, and for **brain→breathing** in the γ band, as well as for IMF3 across all bands except α , during both CBTs compared to **Rest**.

3.3.4 Body→brain

Figure 8 shows that, for both CBTs, G-causal relationships increased for IMFs 2 and 3 across all frequency bands compared to **Rest**; with the greatest increase observed for **breathing→brain** relationships on IMF 3. Additionally, **breathing→brain** relationships increased on IMF 4 in the θ and γ bands; and, in the majority of channels, for **HRV→brain** on IMF 4 in γ . In contrast, **HRV→brain** relationships decreased on IMF 4 in the θ , α and β bands, and on IMF 1 in the δ band during **CBT 1**, and the γ band during **CBT 2**. **Breathing→brain** relationships also decreased for IMF 1 in the θ and β bands, as well as in δ band during **CBT 2** and the α band during **CBT 1**.

Interestingly, channel distribution shows that G-causal relationships increased predominantly over central and frontal channels for **HRV→brain** on IMF3 in the θ and γ bands, and for **breathing→brain** in the δ and γ bands during both CBTs compared to **Rest**. However, G-causal relationships increased over temporal, parietal and occipital channels, for **HRV→brain** for IMF3 in the δ and α bands, and for **breathing→brain** in the β and α bands during both CBTs compared to **Rest**.



3.4 Spectral component analysis

Figure 9 presents the BPTs spectral analysis results for **CBT 1**, Figure 10 for **CBT 2** and Figure 11 for **Rest**. These figures illustrate how, despite EMD being a non-linear decomposition method, each IMF demonstrated a consistent frequency range and content across subjects. Importantly, because EMD is a data-driven method, it does not rely on predefined frequency bands or filtering assumptions. This allows the extracted IMFs to reflect intrinsic oscillatory dynamics rather than imposed spectral boundaries. Furthermore, IMF 3 displayed a clear relationship with each **CBT** (Figures 9, 10), exhibiting a peak in all frequency bands, except for θ , centered at the respective **CBT** frequency.

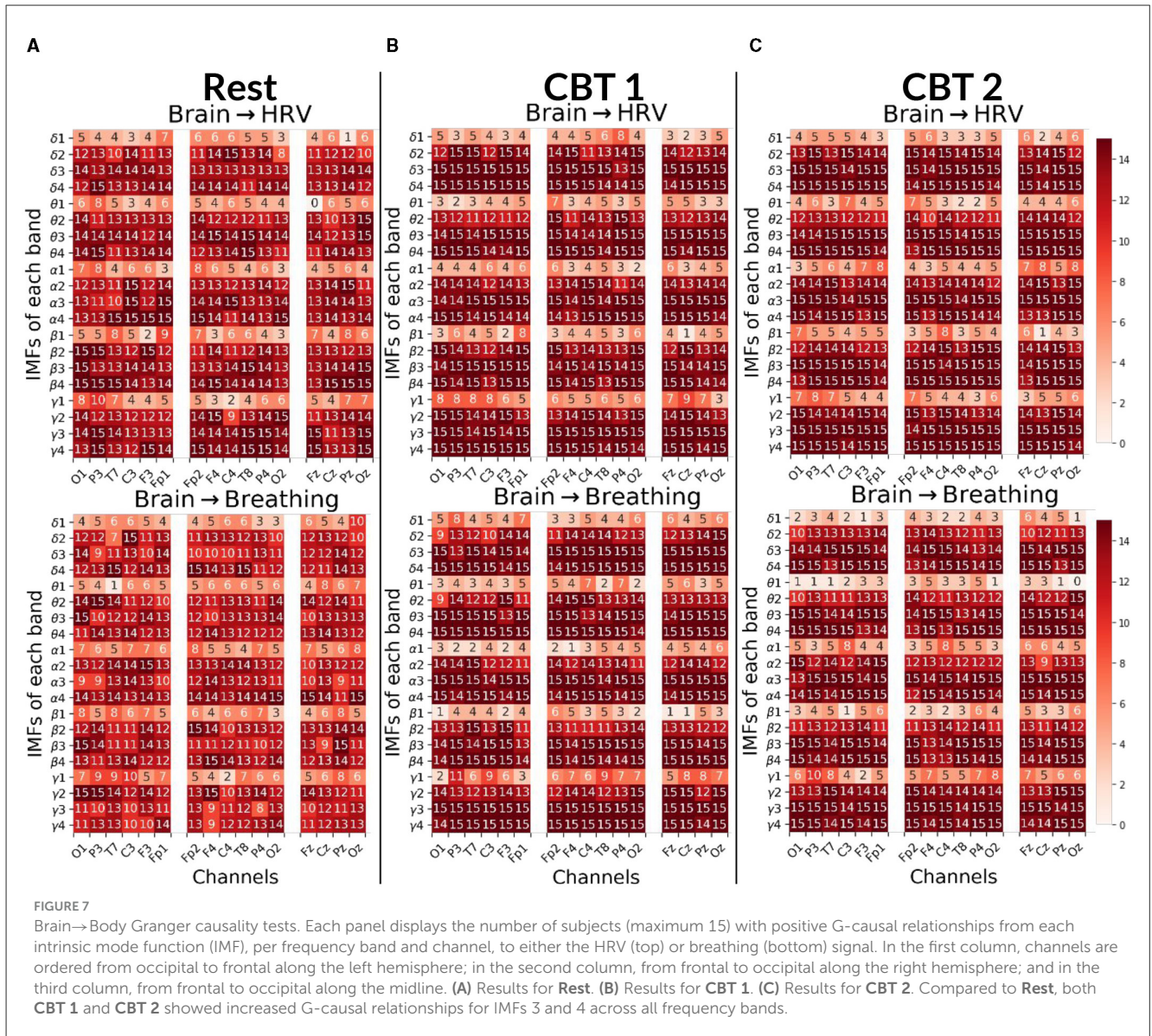
For each IMF and frequency band from the Cz channel, a cross-correlation analysis was performed with each subject's breathing signal. The respective IMF was adjusted to the optimal lag, and the resulting Pearson's coefficient between the signals was calculated. The highest average correlation across subjects was observed for IMF 3 in the γ band during **CBT 2**, with a value of 0.307, indicating a weak correlation, which suggests a less direct or potentially artificial relationship with the physical phenomenon. Nonetheless, both signals shared a similar dominant frequency, suggesting that IMF 3 still captured oscillatory dynamics temporally aligned with the breathing rhythm, thereby supporting the notion of frequency-based coupling even in the absence of strong amplitude correlation.

Notably, Figure 9F reveals a secondary peak in IMF 4 centered at ~ 0.15 Hz, which was observed only in the γ band during

CBT 1. According to Klimesch (2018) binary hierarchy model, this frequency (~ 0.16 Hz) represents one of three preferred breathing rates linked to different affective and cognitive states (Klimesch, 2018; Pfurtscheller et al., 2025). While the dominant frequency in **CBT 1** corresponds to the instructed breathing rhythm (~ 0.05 Hz), the emergence of a peak near 0.15 Hz may reflect an endogenous modulation mechanism operating within a harmonically related frequency range, as predicted by the binary hierarchy model.

The PSD of the breathing signal reveals a distinct cyclical phenomenon in both **CBTs** (Figures 9A, 10A), with the highest peak centered around the respective **CBT** frequency, followed by smaller peaks at subsequent harmonics. This pattern indicates that the controlled breathing exercise was effectively performed in both conditions. Furthermore, after adjusting each subject's breathing signal based on the optimal lag identified through cross-correlation with the respective **CBT**, the average Pearson's correlation coefficients across subjects were 0.82 for **CBT 1** and 0.81 for **CBT 2**. In this context, a high correlation could indicate both accurate performance of the **CBT** and adequate estimation of the breathing signal.

Furthermore, the PSD of the breathing signal during the **Rest** condition (Figure 11) showed spectral peaks centered around ~ 0.1 Hz and ~ 0.32 Hz. These spontaneous breathing rates align with previously reported patterns observed in both healthy participants and patients undergoing MRI sessions (Pfurtscheller et al., 2019, 2025; Zelano et al., 2016). The presence of a ~ 0.32 Hz peak is consistent with one of the preferred breathing frequencies proposed by the binary hierarchy model (Klimesch, 2018), suggesting that



even in resting conditions, participants may exhibit spontaneous breathing rhythms with functional significance.

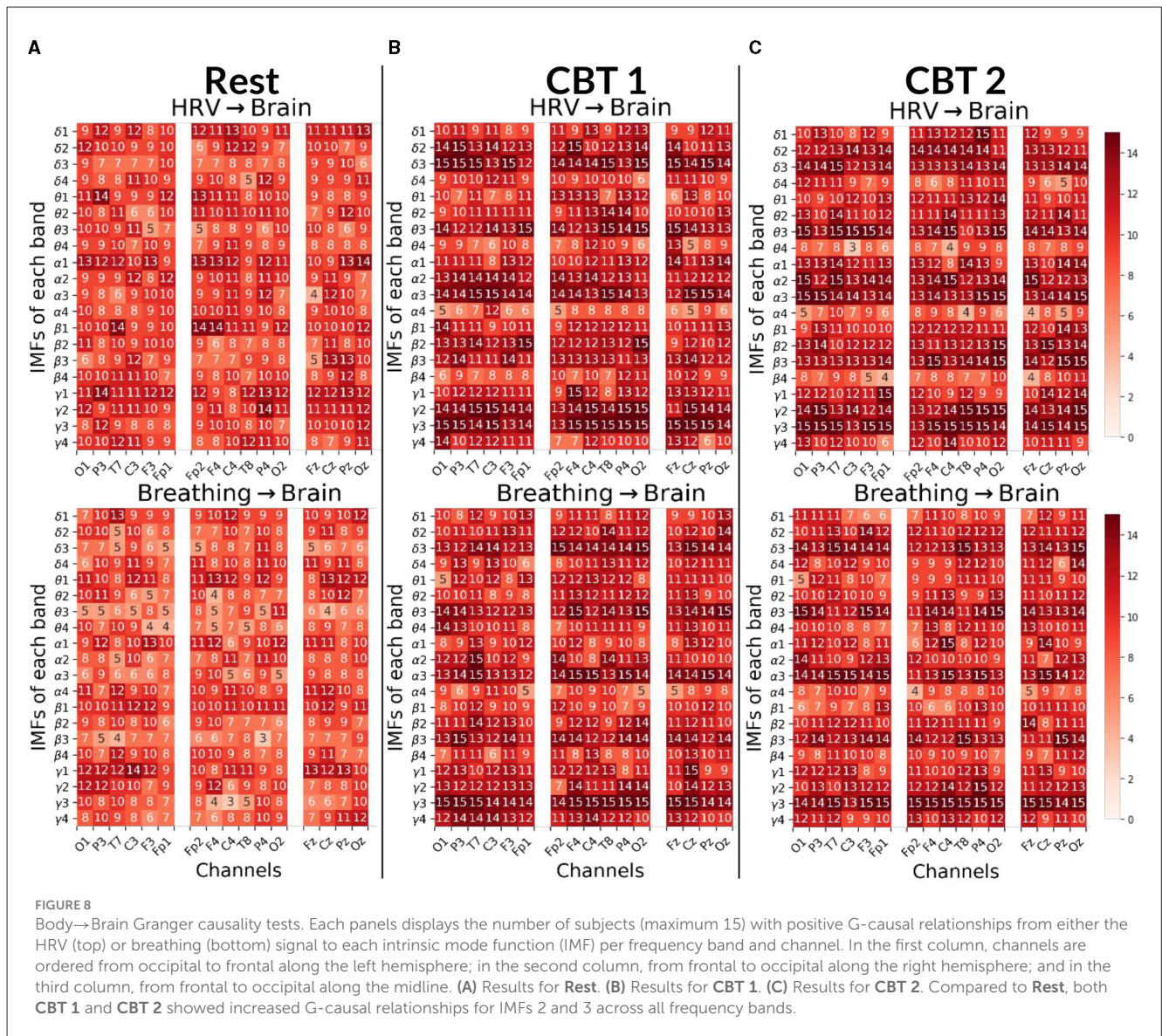
4 Discussion

The primary finding of this study is the observation of bidirectional G-causal relationships between brain BPTs and autonomic events, specifically HRV and breathing, during CBTs. The decomposition of BPTs into IMFs reveals distinct spectral components that are differentially modulated across conditions, suggesting that each IMF reflects varying physiological mechanisms underlying these interactions.

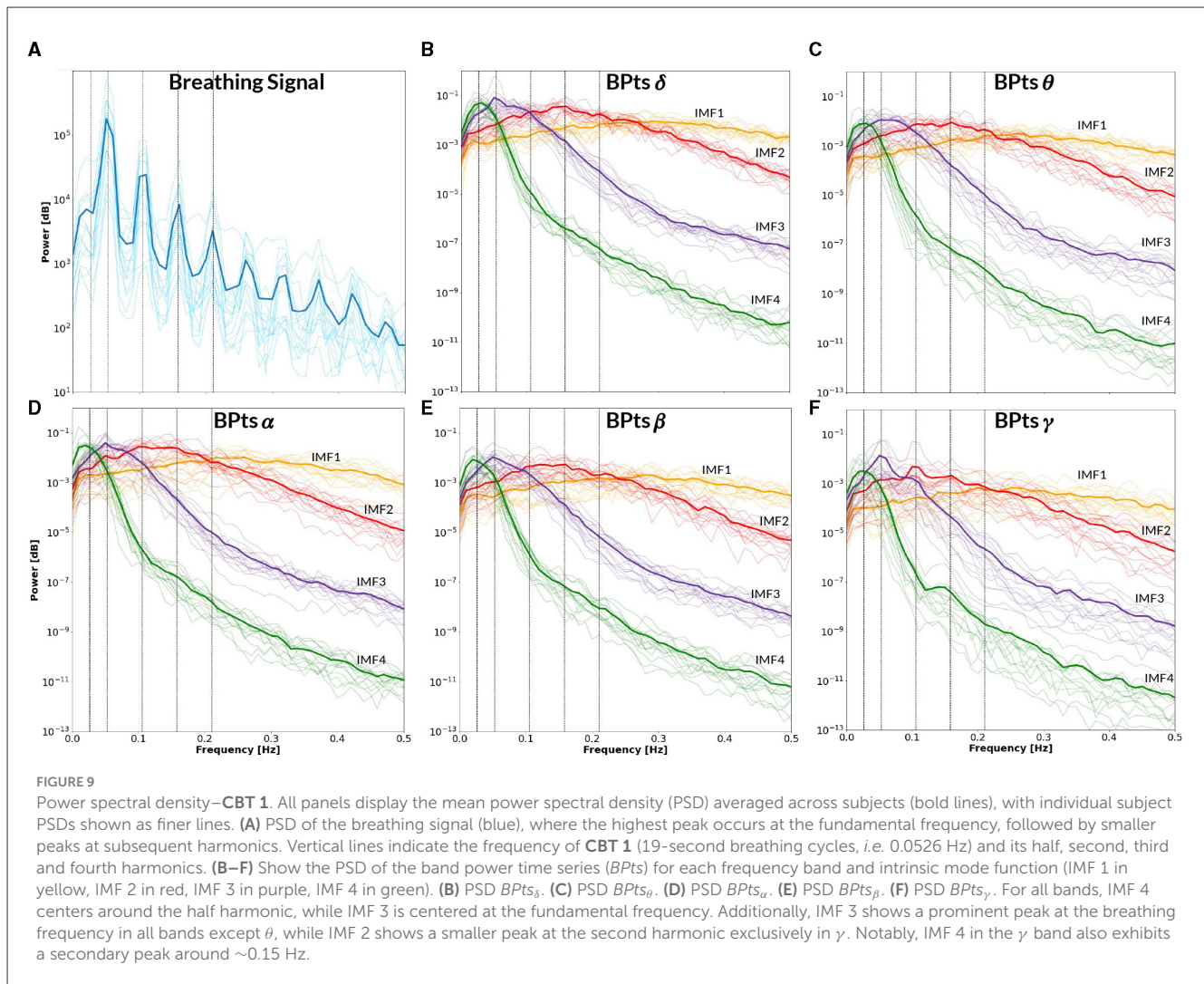
An important consideration when interpreting these results is ensuring the observed G-causal relationships are not experimental artifacts. One compelling argument against this is the consistent positive G-causal relationships observed between HRV and breathing signals across all subjects and conditions, as shown

in Figure 1C. HRV is tightly coupled with breathing via RSA, where RR intervals decrease during inhalation and increase during exhalation (Klimesch, 2018). The bidirectional positive relationships in all subjects confirm their common origin. Additionally, to support the notion that the observed relationships are not artifactual, the low subject-level correlation values, specifically for IMF 1 in Figure 7 and IMF 4 in Figure 8, suggest that the brain↔body G-causal interactions are unlikely to reflect muscular artifacts in the EEG. Moreover, the highest observed cross-correlation between breathing and EEG components (IMF 3 in the γ band during CBT 2) was only 0.307, indicating a weak amplitude coupling. This further supports the idea that frequency alignment, rather than volume-conducted muscle activity, underlies the observed effects.

Further, the decomposition of BPTs into IMFs, in conjunction with the observed G-causal relationships, suggests that brain↔body communication occurs through distinct spectral pathways. Each IMF appears to capture distinct aspects of



the underlying physiological processes, with each spectral feature potentially representing a unique component of the communication between brain and body. This provides

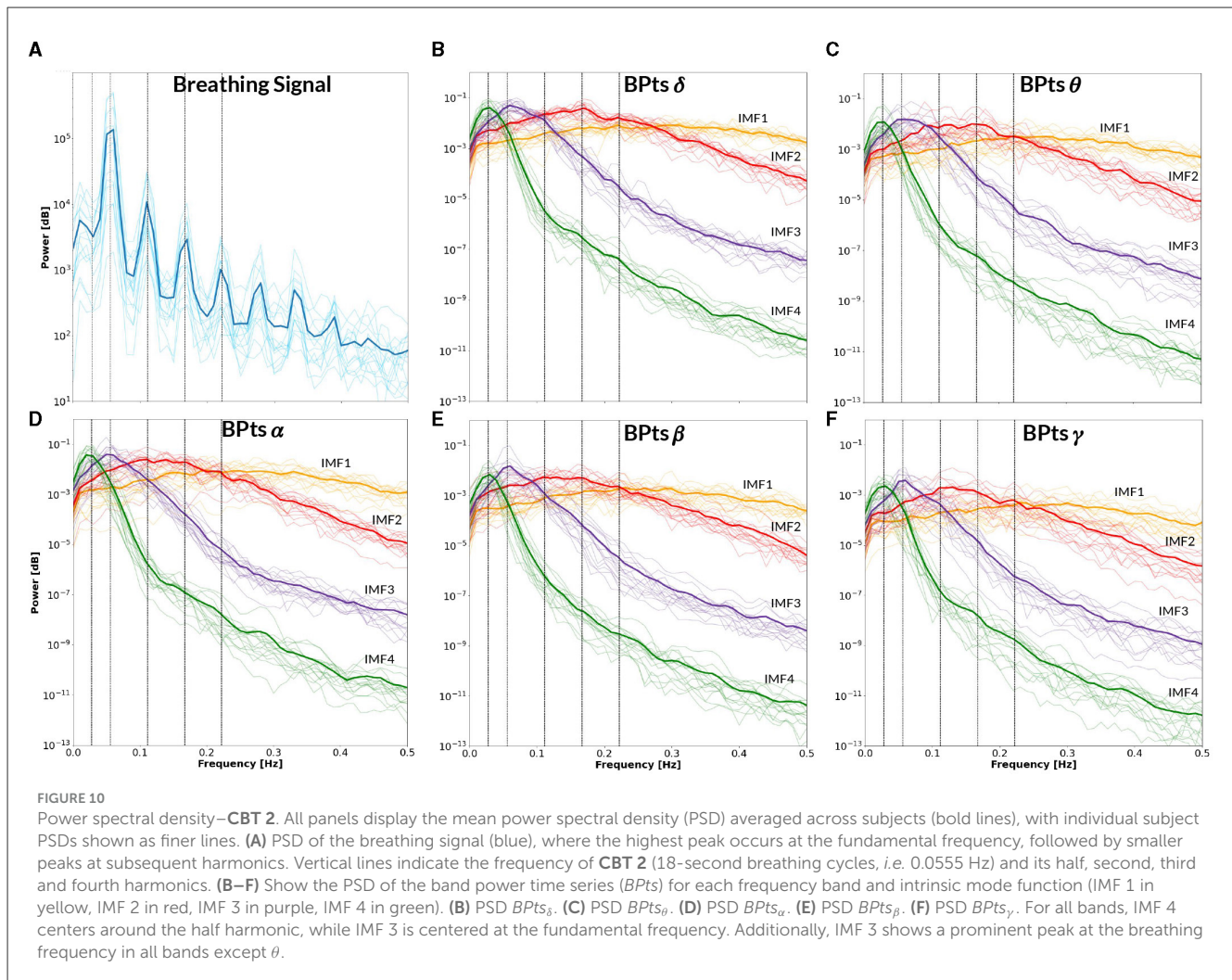


These results are also consistent with earlier findings of our group (Pardo-Rodriguez et al., 2021a), which applied EMD to HRV signals to examine their interaction with BPTs during controlled breathing. That study showed that fast HRV components (like IMF 2) increased Granger causality in the **HRV**→**brain** direction, while slow HRV components (like IMF 4) enhanced causality in the **brain**→**HRV** direction. This differentiation between fast and slow components observed in both studies may reflect distinct temporal mechanisms underlying short-latency autonomic responses and slower, integrative regulatory processes during conscious breathing.

One key aspect of these findings is the prominent role of the γ band in the **body**↔**brain** interactions during CBTs. Significant G-causal relationships in the γ band increased notably during both CBTs, aligning with prior studies that highlight γ rhythms as crucial for inter-regional brain communication, and extending this role to interactions with peripheral systems. For instance, Herrero et al. (2018) showed that during conscious breathing, γ band coherence increases in regions such as the anterior cingulate and premotor cortex, suggesting involvement in coordinating neural processes during rhythmic activities like breathing. Animal studies have found that respiration modulates the amplitude of γ sub-bands in frontal areas, with respiratory activity phase-locking

to neural oscillations, potentially synchronizing brain regions and linking γ rhythms to neural regulation during breathing tasks (Tort et al., 2018, 2025; Zelano et al., 2016). Moreover, γ -band activity has been shown to precede autonomic fluctuations such as heart rate and blood pressure during mental tasks (Umeno et al., 2002), suggesting an anticipatory role in modulating peripheral responses. Pardo-Rodriguez et al. (2021a) also reported increased G-causal relationships in the γ band during a CBT, underscoring the role of high-frequency rhythms in coordinating cortical and autonomic activity. Altogether, these findings suggest that γ oscillations may mediate neuro-autonomic synchronization, potentially bridging central and peripheral systems during conscious breathing. This aligns with broader theories positioning γ band activity as a fundamental mechanism in sensory, cognitive, and physiological regulation (Başar, 2013; Herrmann et al., 2004).

The distribution of G-causal relationships across channels provides valuable insight into the spatial dynamics of **brain**↔**body** interactions during CBTs. During both CBTs, the **brain**→**body** causal relationships were predominantly localized to frontal channels, particularly in the γ band. This frontal predominance suggests that higher-order cognitive and regulatory processes, such as attention and executive control, may play a central role



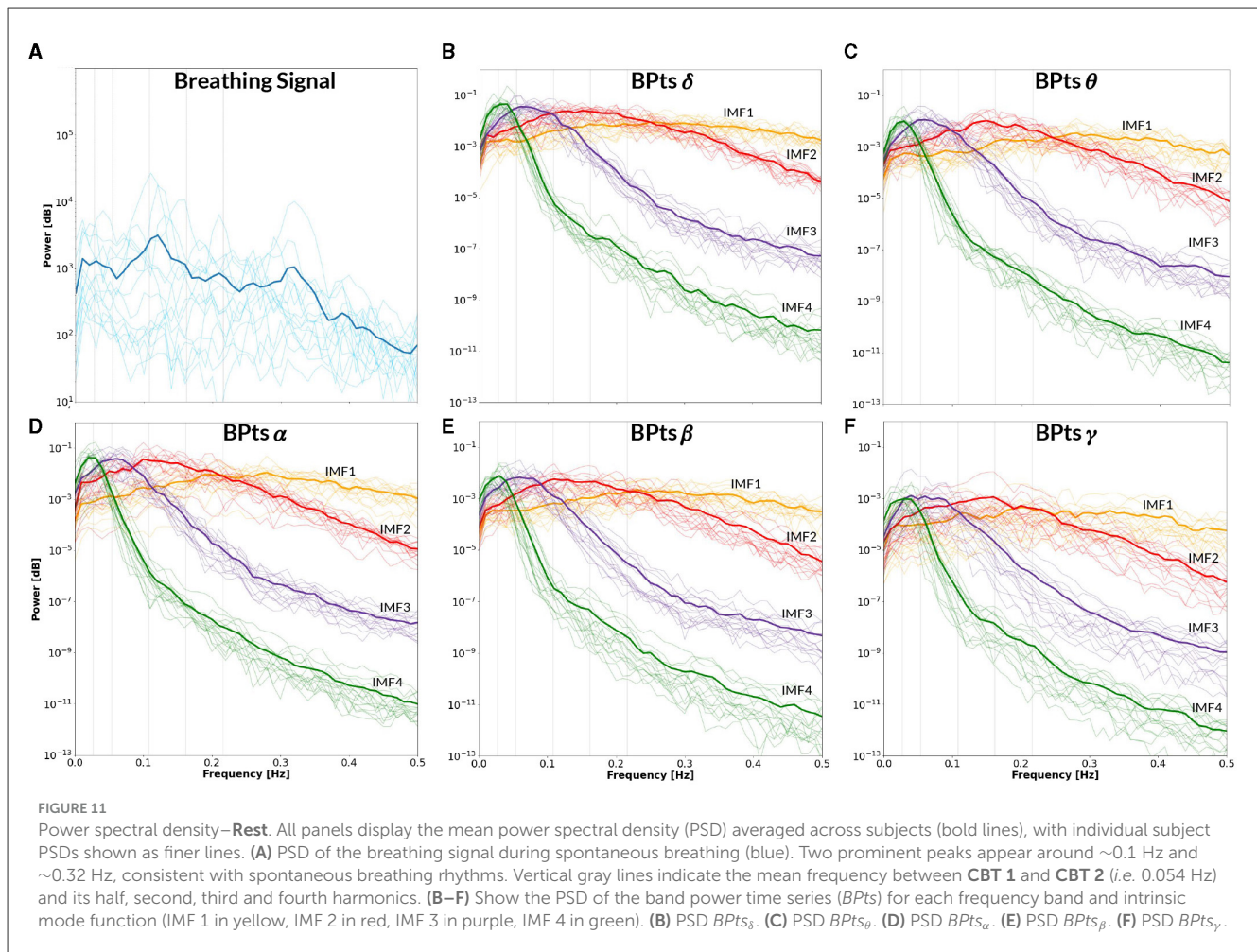
in modulating autonomic responses during controlled breathing (Herrero et al., 2018; Tort et al., 2018). The frontal cortex is involved in regulating both emotional and physiological states, and its engagement in **brain**↔**body** communication during CBTs likely reflects an active closed-loop modulation of autonomic functions in response to the breathing task. This finding resonates with studies showing that prefrontal regions are involved in interoception practices and conscious breathing techniques (Weng et al., 2021), underscoring the role of frontal regions in maintaining control over physiological processes.

Conversely, **body**→**brain** G-causal relationships shifted toward occipital regions, particularly in the δ , β , and α bands. This may reflect the influence of peripheral physiological signals, such as breathing, on cortical regions involved in sensory processing and integration. This finding mirrors our earlier observation (Pardo-Rodriguez et al., 2021a), where shifts from frontal to occipital regions were linked with changes in breathing patterns and peripheral influences, emphasizing the dynamic and flexible nature of **brain**↔**body** communication during CBTs. Additionally, occipital engagement may relate to the neurophysiological mechanisms underlying slow, deep breathing, which can entrain central autonomic networks and optimize HRV through specific

respiratory patterns around 0.1 Hz (Mather and Thayer, 2018; Noble and Hochman, 2019). These breathing-induced shifts may promote coordination between respiratory and sensory processing regions, facilitating the integration of autonomic feedback into cortical areas involved in sensory input and motor coordination.

The widespread increase in BPTs synchrony observed during the CBTs, particularly in the γ band, but also across slower frequencies, suggests that paced breathing may induce large-scale coordination of cortical rhythms. This pattern aligns with the supramodal entrainment framework (Lakatos et al., 2019), which posits that rhythmic input can drive large-scale cortical oscillatory dynamics beyond sensory-specific regions. CBTs may act as a multisensory stimulus—integrating interoceptive (breath), proprioceptive (chest movement), and auditory (cue) inputs—thereby engaging broader sensorimotor and autonomic networks. Supporting this, Tort et al. (2025) has shown that respiration can synchronize neural activity across widespread brain regions, modulating faster oscillations and shaping inter-regional communication.

Interestingly, we observed prominent components at ~ 0.025 Hz (IMF 4) and ~ 0.05 Hz (IMF 3), consistent with infra-slow oscillations (ISOs) reported in animal and human studies. Work



in rodents has shown serotonin fluctuations at these frequencies organize wake and sleep substate transitions (Cooper et al., 2025). In humans, fMRI and ECoG studies have linked ISOs to dynamic hippocampus-cortex communication during rest and sleep (Mitra et al., 2016). Our findings suggest these slow rhythms may also emerge during active, conscious breathing states such as CBTs. This raises the possibility that slow, controlled breathing could entrain or enhance endogenous ISOs, potentially supporting corticocortical interactions involved in emotional regulation and memory-related processes (Tort et al., 2025).

Finally, EEG band power values may show mixed results across resting states and various tasks in several studies. This study found a decrease in $BPTs_{\alpha}$ and $BPTs_{\theta}$ at specific brain regions during both CBTs compared to Rest. Zaccaro et al. (2018) systematic review suggests slow controlled breathing causes decreased θ and increased α power. These results support the notion that controlled breathing can decrease θ activity.

While sex differences in HRV and EEG spectral power are well-documented, the use of relative measures such as BPTs and IMFs inherently minimizes their potential influence. Moreover, the controlled environment including a seated posture and adaptation period was designed to reduce sources of variability and ensure more consistent baseline intersubject measures. When analyzing the data by sex, females showed fewer G-causal relationships for **brain↔breathing** during Rest, but not during

CBTs, suggesting that conscious breathing elicits robust cortical-autonomic interactions across sexes.

Future studies should examine pathological models that isolate or alter **brain↔heart** communication pathways to better understand their origin and rule out analysis-related artifacts. Future analyses could include applying EMD to HRV signals to disentangle sympathetic and parasympathetic contributions, as well as assessing the time course of BPTs synchronization to the breathing rhythm during task onset.

Taken together, these findings reveal that conscious breathing can modulate cortical-autonomic dynamics through frequency-specific neural mechanisms. By showing that neural oscillations particularly in the γ band dynamically synchronize with autonomic rhythms aligned with the breathing frequency, we provide strong support for the neural basis of respiratory entrainment and highlight the brain's active role in flexibly regulating peripheral physiology through distinct spectral pathways. These results contribute to a systems-level perspective on brain-body integration, revealing a dynamic closed-loop interaction essential for maintaining physiological homeostasis and adaptive regulation. This study lays the groundwork for developing breathing-based interventions aimed at enhancing self-regulation, with potential applications in biofeedback, stress management, and improving physiological and mental well-being.

Data availability statement

The raw data supporting the conclusions of this article will be made available by the authors, without undue reservation.

Ethics statement

The studies involving humans were approved by Comité de Ética de la Universidad Iberoamericana Ciudad de México. The studies were conducted in accordance with the local legislation and institutional requirements. The participants provided their written informed consent to participate in this study. Written informed consent was obtained from the individual(s) for the publication of any potentially identifiable images or data included in this article.

Author contributions

MP-R: Data curation, Software, Visualization, Project administration, Conceptualization, Writing – original draft, Formal analysis, Investigation, Validation, Methodology, Writing – review & editing, Resources. EB-V: Software, Formal analysis, Project administration, Funding acquisition, Resources, Methodology, Conceptualization, Validation, Writing – review & editing, Supervision. OA-C: Methodology, Conceptualization, Writing – review & editing, Supervision, Validation. OY-S: Software, Writing – review & editing, Validation, Supervision.

Funding

The author(s) declare that financial support was received for the research and/or publication of this article. This work was supported by the Dirección de Investigación y Posgrado at Universidad Iberoamericana Ciudad de México, which provided resources for equipment acquisition. MariNieves Pardo-Rodriguez received a full doctoral scholarship from Universidad Iberoamericana Ciudad de México and an additional doctoral fellowship from the Secretaría de Ciencia, Humanidades, Tecnología e Innovación (SECIHTI). The funders had no role in study design, data collection and analysis, decision to publish, or preparation of the manuscript.

References

- Al-Ezzi, A., Arechavala, R. J., Butler, R., Nolty, A., Kang, J. J., Shimojo, S., et al. (2024). Disrupted brain functional connectivity as early signature in cognitively healthy individuals with pathological csf amyloid/tau. *Commun. Biol.* 7:1. doi: 10.1038/s42003-024-06673-w
- Ashhad, S., Kam, K., Negro, C. A. D., and Feldman, J. L. (2022). Breathing rhythm and pattern and their influence on emotion. *Annu. Rev. Neurosci.* 45, 223–247. doi: 10.1146/annurev-neuro-090121-014424
- Başar, E. (2013). A review of gamma oscillations in healthy subjects and in cognitive impairment. *Int. J. Psychophysiol.* 90, 99–117. doi: 10.1016/j.ijpsycho.2013.07.005
- Benson, H., Beary, J. F., and Carol, M. P. (1974). The relaxation response. *Psychiatry* 37, 37–46. doi: 10.1080/00332747.1974.11023785
- Bhargava, R., Gogate, M., and Mascarenhas, J. (1988). Autonomic responses to breath holding and its variations following pranayama. *Indian J. Physiol. Pharmacol.* 32:257264.
- Carnevali, L., Sgoifo, A., Trombini, M., Landgraf, R., Neumann, I. D., and Nalivaiko, E. (2013). Different patterns of respiration in rat lines selectively bred for high or low anxiety. *PLoS ONE* 8:e64519. doi: 10.1371/journal.pone.0064519
- Cooper, C., Parthier, D., Sibille, J., Tukker, J. J., Tritsch, N., and Schmitz, D. (2025). Ultraslow serotonin oscillations in the hippocampus delineate substates across nrem and waking. *Elife* 13:101105. doi: 10.7554/eLife.101105.3.sa4
- Critchley, H., and Garfinkel, S. (2015). Interactions between visceral afferent signaling and stimulus processing. *Front. Neurosci.* 9:286. doi: 10.3389/fnins.2015.00286

Acknowledgments

The authors would like to thank the Dirección de Investigación y Posgrado at Universidad Iberoamericana Ciudad de México for providing the resources to acquire the equipment used in this study. We also acknowledge the support of the Secretaría de Ciencia, Humanidades, Tecnología e Innovación (SECIHTI) for awarding a doctoral fellowship to MariNieves Pardo-Rodriguez, as well as Universidad Iberoamericana Ciudad de México for granting her a full doctoral scholarship.

Conflict of interest

The authors declare that the research was conducted in the absence of any commercial or financial relationships that could be construed as a potential conflict of interest.

Generative AI statement

The author(s) declare that Gen AI was used in the creation of this manuscript. This manuscript was edited for language and clarity with the assistance of ChatGPT (OpenAI, GPT-4), under the supervision and full responsibility of the author(s). No interpretations, data analyses, or figure generation were performed using generative AI.

Any alternative text (alt text) provided alongside figures in this article has been generated by Frontiers with the support of artificial intelligence and reasonable efforts have been made to ensure accuracy, including review by the authors wherever possible. If you identify any issues, please contact us.

Publisher's note

All claims expressed in this article are solely those of the authors and do not necessarily represent those of their affiliated organizations, or those of the publisher, the editors and the reviewers. Any product that may be evaluated in this article, or claim that may be made by its manufacturer, is not guaranteed or endorsed by the publisher.

- Critchley, H. D., Nicotra, A., Chiesa, P. A., Nagai, Y., Gray, M. A., Minati, L., et al. (2015). Slow breathing and hypoxic challenge: Cardiorespiratory consequences and their central neural substrates. *PLoS ONE* 10:e0127082. doi: 10.1371/journal.pone.0127082
- De la Cruz-Armenta, V., Bojorges-Valdez, E., and Yanez-Suarez, O. (2017). *Granger Causality Suggests an Association Between Heart Rate Variability and EEG Band Power Dynamics*.
- Faes, L., Greco, A., Lanata, A., Barbieri, R., Scilingo, E. P., and Valenza, G. (2017). "Causal brain-heart information transfer during visual emotional elicitation in healthy subjects: Preliminary evaluations and future perspectives," in *2017 39th Annual International Conference of the IEEE Engineering in Medicine and Biology Society (EMBC)* (Jeju: IEEE), 1559–1562. doi: 10.1109/EMBC.2017.8037134
- Granger, C. W. J. (1969). Investigating causal relations by econometric models and cross-spectral methods. *Econometrica* 37:424. doi: 10.2307/1912791
- Hamilton, P. (2002). "Open source ECG analysis," in *Computers in Cardiology, CIC-02* (Memphis, TN: IEEE).
- Herrero, J. L., Khuvis, S., Yeagle, E., Cerf, M., and Mehta, A. D. (2018). Breathing above the brain stem: volitional control and attentional modulation in humans. *J. Neurophysiol.* 119, 145–159. doi: 10.1152/jn.00551.2017
- Herrmann, C. S., Munk, M. H. J., and Engel, A. K. (2004). Cognitive functions of gamma-band activity: memory match and utilization. *Trends Cogn. Sci.* 8, 347–355. doi: 10.1016/j.tics.2004.06.006
- Huang Norden, E., Zheng, S., Long Steven, R., Wu Manli, C., Shih Hsing, H., Qunan, Z., et al. (1998). The empirical mode decomposition and the hilbert spectrum for nonlinear and non-stationary time series analysis. *Proc. Royal Soc. London. Series A: Mathem. Phys. Eng. Sci.* 454, 903–995. doi: 10.1098/rspa.1998.0193
- Klimesch, W. (2013). An algorithm for the EEG frequency architecture of consciousness and brain body coupling. *Front. Hum. Neurosci.* 7:766. doi: 10.3389/fnhum.2013.00766
- Klimesch, W. (2018). The frequency architecture of brain and brain body oscillations: an analysis. *Eur. J. Neurosci.* 48, 2431–2453. doi: 10.1111/ejn.14192
- Lakatos, P., Gross, J., and Thut, G. (2019). A new unifying account of the roles of neuronal entrainment. *Curr. Biol.* 29:R890R905. doi: 10.1016/j.cub.2019.07.075
- Lakatos, P., Shah, A. S., Knuth, K. H., Ulbert, I., Karmos, G., and Schroeder, C. E. (2005). An oscillatory hierarchy controlling neuronal excitability and stimulus processing in the auditory cortex. *J. Neurophysiol.* 94, 1904–1911. doi: 10.1152/jn.00263.2005
- Mather, M., and Thayer, J. F. (2018). How heart rate variability affects emotion regulation brain networks. *Curr. Opin. Behav. Sci.* 19, 98–104. doi: 10.1016/j.cobeha.2017.12.017
- Mitra, A., Snyder, A. Z., Hacker, C. D., Pahwa, M., Tagliazucchi, E., Laufs, H., et al. (2016). Human cortical/hippocampal dialogue in wake and slow-wave sleep. *Proc. Nat. Acad. Sci.* 113:44. doi: 10.1073/pnas.1607289113
- Molloy, C., Choy, E. H., Arechavala, R. J., Buennagel, D., Nolty, A., Spezzaferri, M. R., et al. (2023). Resting heart rate (variability) and cognition relationships reveal cognitively healthy individuals with pathological amyloid/tau ratio. *Front. Epidemiol.* 3:1168847. doi: 10.3389/fepid.2023.1168847
- Noble, D. J., and Hochman, S. (2019). Hypothesis: Pulmonary afferent activity patterns during slow, deep breathing contribute to the neural induction of physiological relaxation. *Front. Physiol.* 10:1176. doi: 10.3389/fphys.2019.01176
- Pardo-Rodriguez, M., Bojorges-Valdez, E., and Yanez-Suarez, O. (2019). "Causal relationship analysis of heart rate variability and power spectral density time series of electroencephalographic signals," in *2019 Computing in Cardiology Conference (CinC)* (Singapore: IEEE), 1–4.
- Pardo-Rodriguez, M., Bojorges-Valdez, E., and Yanez-Suarez, O. (2021a). Bidirectional intrinsic modulation of EEG band power time series and spectral components of heart rate variability. *Auton. Neurosci.* 232:102776. doi: 10.1016/j.autneu.2021.102776
- Pardo-Rodriguez, M., Bojorges-Valdez, E., and Yanez-Suarez, O. (2021b). "Disruption of the cortical-vagal communication network in Parkinson's disease," in *2021 43rd Annual International Conference of the IEEE Engineering in Medicine & Biology Society (EMBC)* (Mexico: IEEE). doi: 10.1109/EMBC46164.2021.9630751
- Pardo-Rodriguez, M., Bojorges-Valdez, E., and Yanez-Suarez, O. (2021c). "Spectral electroencephalographic and heart rate variability features enhance identification of medicated/non-medicated Parkinson's disease patients," in *2021 43rd Annual International Conference of the IEEE Engineering in Medicine & Biology Society (EMBC)* (Mexico: IEEE). doi: 10.1109/EMBC46164.2021.9629543
- Pfurtscheller, G., Rassler, B., Kaminski, M., Schwarz, G., Andrade, A., Pfurtscheller, K., et al. (2025). Brain-breathing interaction during mri-related anxiety. *Clini. Neurophysiol.* 178:2110961. doi: 10.1016/j.clinph.2025.2110961
- Pfurtscheller, G., Rassler, B., Schwerdtfeger, A. R., Klimesch, W., Andrade, A., Schwarz, G., et al. (2019). "switch-off" of respiratory sinus arrhythmia may be associated with the activation of an oscillatory source (pacemaker) in the brain stem. *Front. Physiol.* 10:939. doi: 10.3389/fphys.2019.00939
- Porges, S. W. (2007). The polyvagal perspective. *Biol. Psychol.* 74, 116–143. doi: 10.1016/j.biopsycho.2006.06.009
- Quinn, A., Lopes-dos Santos, V., Dupret, D., Nobre, A., and Woolrich, M. (2021). Emd: Empirical mode decomposition and hilbert-huang spectral analyses in Python. *J. Open Source Softw.* 6:2977. doi: 10.21105/joss.02977
- Russo, M. A., Santarelli, D. M., and ORourke, D. (2017). The physiological effects of slow breathing in the healthy human. *Breathe* 13, 298–309. doi: 10.1183/20734735.009817
- Saper, C. B. (2002). The central autonomic nervous system: Conscious visceral perception and autonomic pattern generation. *Ann. Rev. Neurosci.* 25, 433–469. doi: 10.1146/annurev.neuro.25.032502.111311
- Shalk, G., McFarland, D. J., Hinterberger, T., Birbaumer, N., and Wolpaw, J. R. (2004). BCI2000: a general-purpose brain-computer interface (BCI) system. *IEEE Trans. Biomed. Eng.* 51, 1034–1043. doi: 10.1109/TBME.2004.827072
- Siegel, M., Donner, T. H., and Engel, A. K. (2012). Spectral fingerprints of large-scale neuronal interactions. *Nat. Rev. Neurosci.* 13, 121–134. doi: 10.1038/nrn3137
- Tort, A. B., Brankak, J., and Draguhn, A. (2018). Respiration-entrained brain rhythms are global but often overlooked. *Trends Neurosci.* 41, 186–197. doi: 10.1016/j.tins.2018.01.007
- Tort, A. B. L., Laplagne, D. A., Draguhn, A., and Gonzalez, J. (2025). Global coordination of brain activity by the breathing cycle. *Nat. Rev. Neurosci.* 26, 333–353. doi: 10.1038/s41583-025-00920-7
- Umeno, K., Hori, E., Tabuchi, E., Takakura, H., Miyamoto, K., Ono, T., et al. (2002). Gamma-band EEGs predict autonomic responses during mental arithmetic. *Auton. Nerv. Syst.* 14, 477–480. doi: 10.1097/00001756-200303030-00036
- Valenza, G., Greco, A., Gentili, C., Lanata, A., Sebastiani, L., Menicucci, D., et al. (2016). Combining electroencephalographic activity and instantaneous heart rate for assessing brain - heart dynamics during visual emotional elicitation in healthy subjects. *Philosoph. Trans. Royal Soc. A: Mathem. Phys. Eng. Sci.* 374:20150176. doi: 10.1098/rsta.2015.0176
- Valenza, G., Mati, Z., and Catrambone, V. (2025). The brainheart axis: integrative cooperation of neural, mechanical and biochemical pathways. *Nat. Rev. Cardiol.* 22, 537–550. doi: 10.1038/s41569-025-01140-3
- Vierra, J., Boonla, O., and Prasertsri, P. (2022). Effects of sleep deprivation and 478 breathing control on heart rate variability, blood pressure, blood glucose, and endothelial function in healthy young adults. *Physiol. Rep.* 10:e15389. doi: 10.14814/phy2.15389
- Weng, H. Y., Feldman, J. L., Leggio, L., Napadow, V., Park, J., and Price, C. J. (2021). Interventions and manipulations of interoception. *Trends Neurosci.* 44, 52–62. doi: 10.1016/j.tins.2020.09.010
- Zaccaro, A., Piarulli, A., Laurino, M., Garbella, E., Menicucci, D., Neri, B., et al. (2018). How breath-control can change your life: a systematic review on psycho-physiological correlates of slow breathing. *Front. Hum. Neurosci.* 12:353. doi: 10.3389/fnhum.2018.00353
- Zelano, C., Jiang, H., Zhou, G., Arora, N., Schuele, S., Rosenow, J., et al. (2016). Nasal respiration entrains human limbic oscillations and modulates cognitive function. *J. Neurosci.* 36, 12448–12467. doi: 10.1523/JNEUROSCI.2586-16.2016
- Zhong, W., Ciatipis, M., Wolfenstetter, T., Jessberger, J., Miller, C., Ponsel, S., et al. (2017). Selective entrainment of gamma subbands by different slow network oscillations. *Proc. Nat. Acad. Sci.* 114, 4519–4524. doi: 10.1073/pnas.1617249114